

Growth and optical properties of III-nitride semiconductors for deep UV (230–350 nm) light-emitting diodes (LEDs) and laser diodes (LDs)

Hideki Hirayama, Atsuhiko Kinoshita,* and Yoshinobu Aoyagi
Semiconductors Laboratory, RIKEN

For the first time, we demonstrated intense ultraviolet (UV) emission at 230–350 nm from III-nitride compound semiconductors grown by metalorganic vapor phase epitaxy (MOVPE). First, we obtained 230 nm-band intense UV emission from $\text{AlN}/\text{Al}_x\text{Ga}_{1-x}\text{N}$ quantum wells (QWs) at 77 K. The emission efficiency of AlGa_xN-based QWs was as high as that of blue light-emitting diodes (LEDs) at low temperature, however, it was not significantly high at room temperature (R.T.). We succeeded in the drastic enhancement of R.T. UV emission, by introducing approximately 5% of In into AlGa_xN, which was due to the efficient radiative recombination of a localized electron-hole pair in In segregation regions. We obtained the first R.T. intense emission of the 320 nm-band from InAlGa_xN-based QWs. The emission intensity of the InAlGa_xN-based QWs was as strong as that of commercially available InGa_xN QWs at R.T. The carrier confinement in the In segregation region was clearly observed from cathode luminescence (CL) measurement. We also achieved p-type doping into wide-bandgap AlGa_xN using several new methods and accomplished the first successful operation of a 330 nm-band LED.

Introduction

GaN and III-nitride compound semiconductors are attracting considerable attention for the realization of visible or ultraviolet (UV) laser diodes (LDs) and light-emitting diodes (LEDs). Blue LDs and violet, blue and green LEDs are already commercially available.¹ In particular, AlGa_xN is expected to be applied in deep UV LDs and bright LEDs, because the direct transition energy can be adjusted between 6.2 eV (AlN) and 3.4 eV (GaN). Figure 1 shows the relationship between the direct transition energy and the lattice constant of wurtzite (Al,Ga,In)N alloy. The emission wavelength

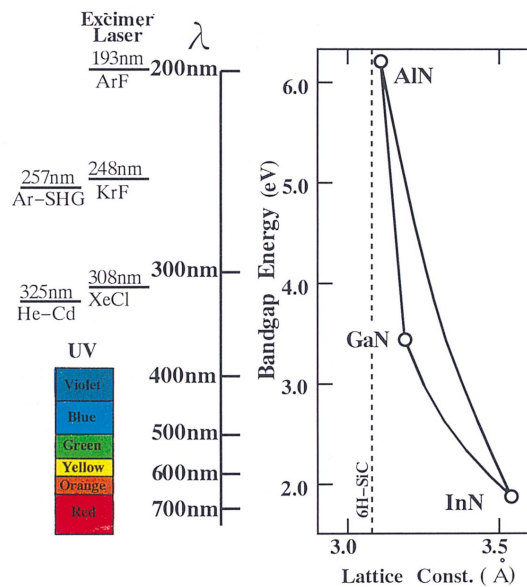


Fig. 1. Relationship between the direct transition energy and the lattice constant of wurtzite (Al,Ga,In)N and wavelength of various UV laser.

* Present address: Department of Chemical Engineering, Waseda University

range of GaN and related materials covers the red to deep UV region, which can be realized by excimer lasers, He-Cd laser or solid-state SHG lasers. Deep UV LDs or LEDs are useful for realizing large-capacity optical memories or long-lifetime fluorescent light. Moreover, they are important in the biochemical and medical fields. However, there are some severe technical problems that prevent realization of UV optical devices. The most serious problems are difficulty in obtaining efficient UV emission from AlGa_xN quantum wells (QWs), in contrast to InGa_xN QWs,¹ as well as the difficulty in achieving p-type doping in high-Al-content AlGa_xN.

First, we studied the growth and optical properties of high-Al-content AlGa_xN. We obtained single-peak emission of Al_xGa_{1-x}N over the entire compositional range, *i.e.*, from GaN to AlN, from near the band edge.² We obtained the shortest wavelength (208 nm) photoluminescence (PL) of a semiconductor from AlN grown on SiC. We also demonstrated the shortest wavelength efficient UV emission at 230–250 nm from AlN(AlGa_xN)/AlGa_xN multi- (M-)QWs.³ The 200 nm-band emissions from AlGa_xN QWs were as strong as those from commercially available InGa_xN QWs at 77 K,³ however, they were weak at room temperature (R.T.).

For the purpose of obtaining R.T. bright UV emission and high hole conductivity of wide-bandgap AlGa_xN, we propose the use of the emission from a localized electron-hole pair in the In segregation region in InAlGa_xN quaternary. It was reported that the quantum-dot-like region formed by In segregation in InGa_xN QWs is very effective for the suppression of nonradiative recombination and that an InGa_xN QW emits well at room temperature.^{4,5} It was also reported that the In content segregation of more than 5% in InGa_xN is necessary for high-current injection devices such as LDs. We need a high Al content ranging from 40 to 60% in order to achieve 300 nm-band-emitting InAlGa_xN quaternary with 5% In incorporation, because of the very large band bowing of InAlGa_xN. We report on the growth and optical properties of InAlGa_xN quaternary and demonstrate R.T. intense deep-UV

emission at 300–340 nm from $\text{In}_x\text{Al}_y\text{Ga}_{1-x-y}\text{N}$ quaternary QWs for the first time.^{6,7)}

As for the current injection of deep-UV-emitting QWs, we have already realized 333 nm current injection emission using Mg-doped GaN/AlGa_xN superlattice (SL) hole conducting layers.⁸⁾ We report on the possibility of p-type doping for wider bandgap AlGa_xN by introducing In.

Experimental details and discussions

Structures were grown at 76 Torr on the Si-face of an on-axis 6H-SiC(0001) substrate by low-pressure (76Torr) metalorganic vapor phase epitaxy (MOVPE). The layer structures consisting of GaN, $\text{Al}_x\text{Ga}_{1-x}\text{N}$, $\text{In}_x\text{Ga}_{1-x}\text{N}$ or $\text{In}_x\text{Al}_y\text{Ga}_{1-x-y}\text{N}$ were grown on a several-hundred-nm-thick $\text{Al}_x\text{Ga}_{1-x}\text{N}$ ($x = 0.1-0.5$) buffer layer which was grown on SiC under optimized growth conditions in order to achieve a flat surface suitable for the WQ layer growth and to reduce the threading dislocation density (TDD). As precursors, ammonia (NH_3), trimethylaluminum (TMAI), trimethylgallium (TMGa), trimethylindium di-*i*-propylamine adduct (TMI-adduct), tetraethylsilane (TESi), and bisethylcyclopentadienylmagnesium (BECp_2Mg) were used with H_2 and N_2 carrier gas. The typical growth temperatures of GaN, $\text{Al}_x\text{Ga}_{1-x}\text{N}$, $\text{In}_x\text{Ga}_{1-x}\text{N}$, and $\text{In}_x\text{Al}_y\text{Ga}_{1-x-y}\text{N}$ are 1000–1100°C, 1050–1250°C, 650–800°C, and 800–870°C, respectively. The typical growth rates of GaN, $\text{Al}_x\text{Ga}_{1-x}\text{N}$, $\text{In}_x\text{Ga}_{1-x}\text{N}$, and $\text{In}_x\text{Al}_y\text{Ga}_{1-x-y}\text{N}$ are 2.4 μm/hour, 0.5–2.4 μm/hour, 0.1 μm/hour and 0.12 μm/hour, respectively.

First, we show the optical properties of AlGa_xN. Figure 2 shows the PL spectra of $\text{Al}_x\text{Ga}_{1-x}\text{N}$ films over the entire Al compositional range, *i.e.*, from GaN to AlN, emitting from near the band edge measured at 77 K. The AlGa_xN alloy was grown directly on a very thin (~5 nm) AlN layer deposited on SiC. The thickness of AlGa_xN film was approximately 250 and 400 nm for AlN and $\text{Al}_{0.11}\text{Ga}_{0.89}\text{N}$, respectively. As seen in Fig. 1, single-peak spectra were obtained for the entire Al compositional range emitting from near the band edge.²⁾ We obtained the first PL emission of AlN and record the shortest wavelength (208 nm) PL of a semiconductor. The deep level yellow emission at approximately 500–550 nm was negligible

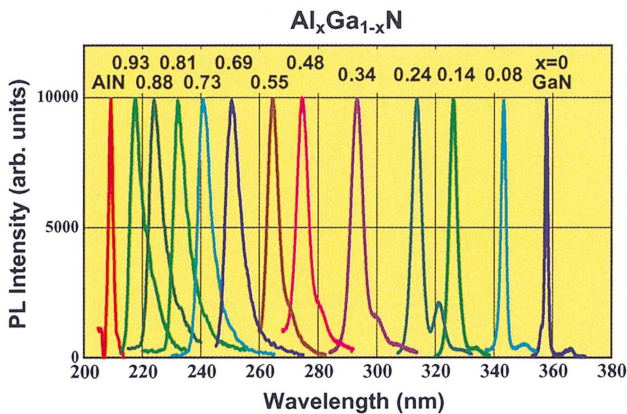


Fig. 2. PL spectra of $\text{Al}_x\text{Ga}_{1-x}\text{N}$ films over the entire Al compositional range, *i.e.*, from GaN to AlN, emitting from near the band edge, measured at 77 K.

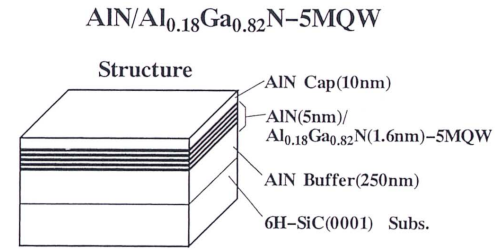


Fig. 3. Schematic layer structure and PL spectra for various quantum well thicknesses of fabricated $\text{AlN}/\text{Al}_{0.18}\text{Ga}_{0.82}\text{N}$ MQW samples.

even for high-Al-content AlGa_xN, indicating the good crystal quality of AlGa_xN.

Then, we fabricated several series of AlGa_xN MQW samples, consisting of various Al-content AlGa_xN barriers. Figure 3 shows the schematic layer structure and the PL spectra for various QW thicknesses of fabricated $\text{AlN}/\text{Al}_{0.18}\text{Ga}_{0.82}\text{N}$ MQW samples. In order to achieve a flat surface suitable for the growth of AlGa_xN quantum wells, an approximately 250–400 nm-thick AlN buffer layer was deposited. We confirmed a step-flow grown surface by atomic force microscopy (AFM). The PL measurement was performed with excitation by a Xe-lamp light source (215 nm) measured at 77 K. We obtained single-peak intense PL emission from each MQW. The most efficient emission was obtained at a wavelength of 234 nm. This is the shortest intense UV emission of a semiconductor QW. The optimum value of well thickness was approximately 1.6 nm. The PL intensity of the MQWs was several tens of times higher than that of bulk AlGa_xN. The quantized level shift was clearly observed. A rapid reduction in the PL intensity with an increase in the well thickness was caused by a reduction in the radiative recombination probability due to a large piezoelectric field in the well.

The PL intensities were compared among AlN/AlGa_xN, AlGa_xN/GaN and InGa_xN/InGa_xN MQWs under the same measurement conditions, as shown in Fig. 4. We found that the PL intensity of 230 nm-band emission from AlGa_xN-based QWs was as strong as that of 420 nm-band emission from commercially available InGa_xN-based QWs, and much stronger than that from GaN-based QWs at 77 K. However, at room temperature, the emissions from AlGa_xN and GaN QWs were much weaker than that from InGa_xN QWs. Thus, the next purpose was to obtain efficient UV emission at room temperature.

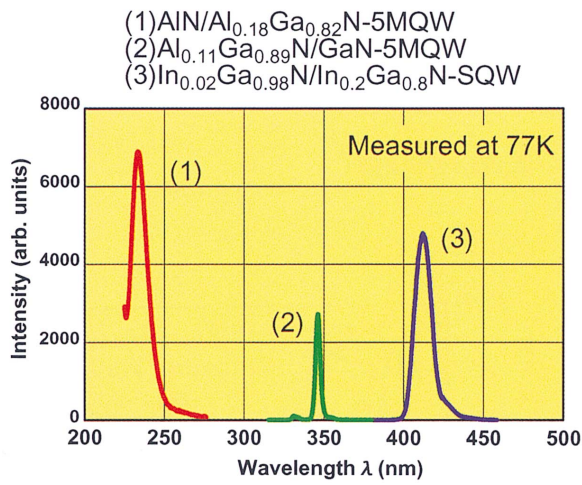


Fig. 4. Comparison of PL intensities among AlN/AlGaIn, AlGaIn/GaN, and InGaIn/InGaIn MQWs under the same measurement conditions.

We introduced several percent of In into AlGaIn alloy to obtain R.T. bright UV emission. We attempted to use the efficient radiative recombination of the localized electron-hole pair in the In segregation region in InAlGaIn quaternary. However, there was no examination of the growth conditions of InAlGaIn quaternary as a strong UV emitter. Thus, we studied the growth conditions of InAlGaIn.

Figure 5 shows PL spectra of 120-nm-thick InGaIn and $In_xAl_yGa_{1-x-y}N$ quaternary for various TMAI flow rates measured at 77 K. The emission of InGaIn grown at 830°C was weak because of the small amount of In incorporation due to too high growth temperature for InGaIn. On the other hand, we found that the InGaIn emission was rapidly enhanced by the Al incorporation. The emission enhancement was due to the increase in In incorporation, which was induced by the increase in Al molar flux. The In content of $In_xGa_{1-x}N$ was 2.2%, and the In, Al, and Ga contents of $In_xAl_yGa_{1-x-y}N$ for a TMAI flow rate of 0.4 sccm were 4.8%, 34.0%, and 61.2%, respectively, measured by a Rutherford backscattering spectrometry (RBS). The R.T. emission intensity of $In_{0.05}Al_{0.34}Ga_{0.61}N$ was as strong as that of $In_{0.2}Ga_{0.8}N$ with the same growth thickness. The full-width at half-maximum (FWHM) of XRD locking curves of InAlGaIn films was as small as that of InGaIn, indicating the good crystal quality of InAlGaIn. Moreover, we found that the emission intensity of

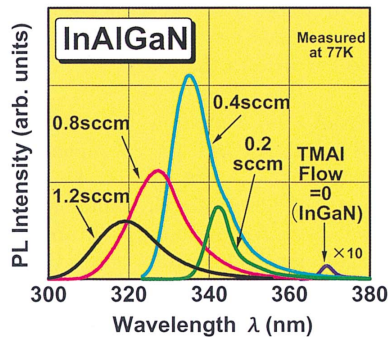


Fig. 5. PL spectra of 120-nm-thick InGaIn and InAlGaIn quaternary for various TMAI flow rates measured at 77 K.

AlGaIn was dramatically enhanced by several percent incorporation of In. The crystal quality was markedly improved by the incorporation of a small amount of In into AlGaIn, which was confirmed by XRD measurement. Furthermore, the non-radiative recombination appears to be markedly reduced by the effect of In segregation as discussed later.

Figure 6 shows the schematic layer structure and the R.T. PL spectra of fabricated InAlGaIn MQW structures measured for various well thicknesses. The structure consisted of a $Al_{0.15}Ga_{0.85}N$ buffer layer, 50 nm-thick $In_{0.02}Al_{0.60}Ga_{0.38}N$ buffer with a thin $In_{0.05}Al_{0.34}Ga_{0.61}N$ strain reducer, $In_{0.05}Al_{0.34}Ga_{0.61}N/In_{0.02}Al_{0.60}Ga_{0.38}N$ three-layer MQW and a 20 nm-thick $In_{0.02}Al_{0.60}Ga_{0.38}N$ cap. All layers were undoped. The samples were excited with an Ar-SHG laser (257 nm). We obtained an intense PL emission for each MQW. The emission intensity of QW was 1 order of magnitude higher than that of bulk quaternary. The most intense PL emission was obtained at 318 nm when the well thickness was approximately 1.4 nm. The emission obtained from the quaternary QW was as strong as that obtained from the InGaIn QW at R.T. In order to observe the localized carrier in In segregation regions, we measured the cathode-luminescence (CL) pattern of an InAlGaIn single (S)QW. We obtained a similar CL pattern from the InAlGaIn SQW as that from the InGaIn SQW, and confirmed the electron-hole localization in the submicron-size In segregation regions in the InAlGaIn SQW.

Figure 7 shows a comparison of the temperature dependencies of PL intensity among InAlGaIn, InGaIn, GaIn, and AlGaIn QWs. The PL intensities of InAlGaIn and InGaIn QWs were

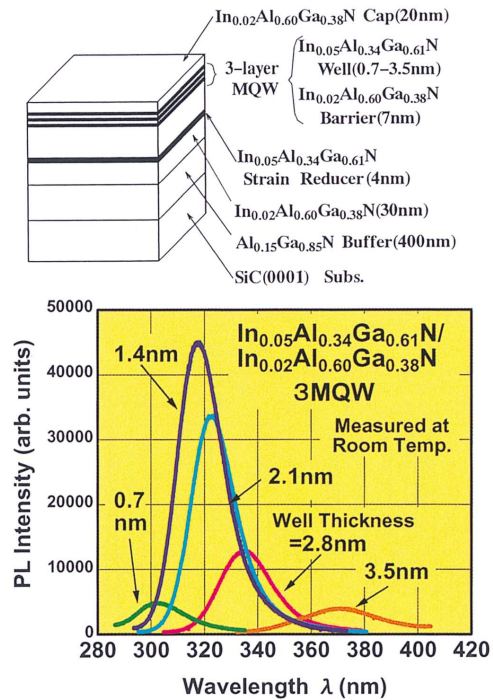


Fig. 6. Schematic layer structure and R.T. PL spectra of fabricated $In_{0.05}Al_{0.34}Ga_{0.61}N/In_{0.02}Al_{0.60}Ga_{0.38}N$ three-layer MQW structures with various well thicknesses.

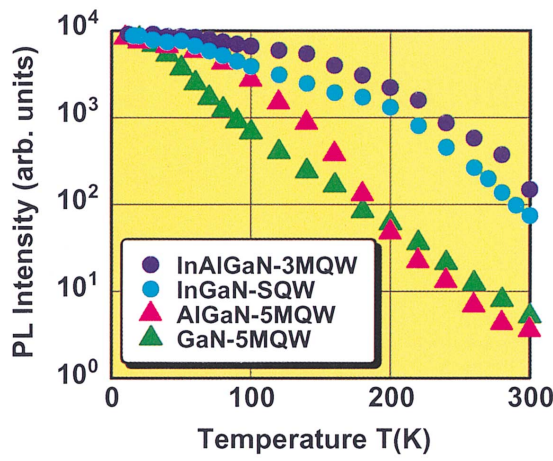


Fig. 7. Comparison of temperature dependencies of PL intensity among InAlGaN, InGaN, GaN, and AlGaIn based-QWs.

1–2 orders of magnitude larger than those of GaN and AlGaIn QWs at R.T. The R.T. emission efficiency of the QW was considered to be markedly improved due to the radiative recombination of the localized electron-hole pair in the In segregation region, as observed by CL measurement. Moreover, the activation energy of the acceptor could be reduced by the effect of a large piezoelectric field applied in In segregation regions. Recently, we grew Mg-doped InAlGaIn under the same growth conditions. We obtained a hole concentration of $3 \times 10^{17} \text{ cm}^{-3}$ by Hall measurement for $\text{In}_{0.05}\text{Al}_{0.50}\text{Ga}_{0.45}\text{N}$, in spite of such a high Al content. From these results, it was shown that the InAlGaIn quaternary is very promising for use as active layers of 300–350 nm-band LDs or LEDs.

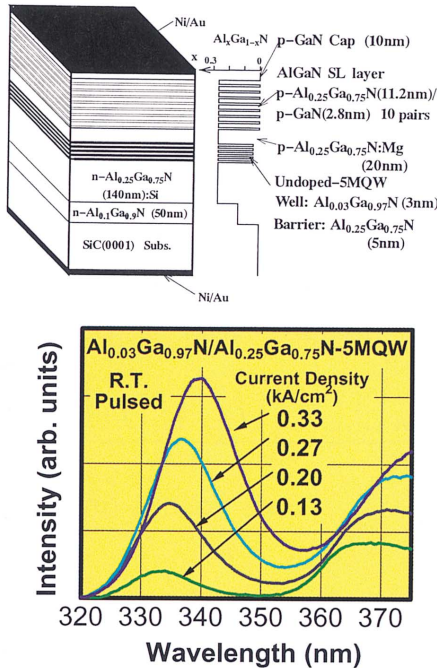


Fig. 8. Schematic structure and current injection spectra of fabricated UV LED operating at the 330 nm band.

Figure 8 shows the schematic structure and the current injection spectra of the fabricated UV LED operating at the 330 nm band. It was very difficult to obtain a hole conductivity for high-Al-content (more than 30%) AlGaIn. We used a Mg-doped AlGaIn/GaN superlattice (SL) structure in order to improve the hole conductivity of a p-type cladding layer. In this example, we used a five-layer $\text{Al}_{0.03}\text{Ga}_{0.97}\text{N}/\text{Al}_{0.25}\text{Ga}_{0.75}\text{N}$ QW structure for emitting regions. We obtained 330–340 nm UV emission at R.T. by pulsed current injection. This is the operation of the shortest wavelength UV LED. The peak of the spectrum was redshifted with increasing injection current due to the heating of emitting layers. The FWHM of the emission spectrum was not changed, indicating that carrier filling did not occur and more intense emission was possible without thermal effects. By changing the active and p-type cladding layers to InAlGaIn-based QWs and SL, 300–330 nm bright LEDs and LDs will be realized.

Conclusions

We demonstrated intense UV emission at 230–350 nm from QW structures consisting of III-nitride semiconductors grown by MOVPE. We obtained 230 nm-band intense UV emission from $\text{AlN}/\text{Al}_x\text{Ga}_{1-x}\text{N}$ QWs at 77 K. The emission efficiency of AlGaIn-based QW was as high as that of blue LEDs at a low temperature, however, at R.T., it was not significantly high. Then, we introduced In into AlGaIn to improve R.T. emission efficiency by the radiative recombination of the localized electron-hole pair in In segregation regions. The efficiency of R.T. UV emission was dramatically enhanced by introducing several percent of In into AlGaIn. We obtained 320 nm-band R.T. intense emission from InAlGaIn/InAlGaIn QWs. The emission intensity of the InAlGaIn-based QW was as strong as that of commercially available InGaIn QWs at R.T. We also achieved p-type doping into wide-bandgap AlGaIn using several methods and accomplished the first successful operation of a 330 nm-band LED. From these results, it was shown that the InAlGaIn quaternary was very promising for use as active layers of 300–350 nm-band LDs or LEDs.

References

- 1) S. Nakamura, M. Senoh, S. Nagahama, N. Iwasa, T. Yamada, T. Matsushita, Y. Sugimoto, and H. Kiyoku: *Jpn. J. Appl. Phys.*, **36**, L1059 (1997).
- 2) H. Hirayama, Y. Enomoto, A. Kinoshita, A. Hirata, and Y. Aoyagi: *Mater. Res. Soc. Symp. Proc.* **595**, W11.35 (1999).
- 3) H. Hirayama, Y. Enomoto, A. Kinoshita, A. Hirata, and Y. Aoyagi: *Phys. Status Solidi A* **180**, 157 (2000).
- 4) Y. Narukawa, Y. Kawakami, M. Funato, S. Fujita, S. Fujita, and S. Nakamura: *Appl. Phys. Lett.*, **70**, 891 (1997).
- 5) S. Chichibu, T. Azuhata, T. Sota, and S. Nakamura: *Appl. Phys. Lett.*, **70**, 2822 (1997).
- 6) H. Hirayama, Y. Enomoto, A. Kinoshita, A. Hirata, and Y. Aoyagi: *Proc. 10th Int. Conf. on Metalorganic Vapor Phase Epitaxy (ICMOVPE-X)*, Fr-A8, Sapporo, 2000–6 (2000).
- 7) H. Hirayama, A. Kinoshita, T. Yamanaka, A. Hirata, and Y. Aoyagi: *Mater. Res. Soc. Symp. Proc.* **G2.8** (2001).
- 8) A. Kinoshita, H. Hirayama, M. Aino, A. Hirata, and Y. Aoyagi: *Appl. Phys. Lett.*, **77**, 175 (2000).